A transient brain endothelial translatome response to endotoxin is associated with mild cognitive changes post-shock in young mice.

Shuhan Lu[1], Iria Di John Portela[1], Nina Martino[1], Ramon Bossardi Ramos[1], Abigail E Salinero[2], Rachel M Smith[2], Kristen L Zuloaga[2], Alejandro P Adam[1,3,4]

1 Department of Molecular and Cellular Physiology, Albany Medical College.

2 Department of Neuroscience & Experimental Therapeutics, Albany Medical College.

3 Department of Ophthalmology, Albany Medical College.

4 To whom correspondence should be addressed at 43 New Scotland Ave, Albany, NY 12208. Adama1@amc.edu

Running title: Brain endothelial transcription during systemic inflammation

Abstract

Sepsis-associated encephalopathy (SAE) is a common manifestation in septic patients that is associated with increased risk of long-term cognitive impairment. SAE is driven, at least in part, by brain endothelial dysfunction in response to systemic cytokine signaling. However, the mechanisms driving SAE and its consequences remain largely unknown. Here, we performed translating ribosome affinity purification and RNA-sequencing (TRAP-seq) from the brain endothelium to determine the transcriptional changes after an acute endotoxemic (LPS) challenge. LPS induced a strong acute transcriptional response in the brain endothelium that partially correlates with the whole brain transcriptional response and suggested an endothelial-specific hypoxia response. Consistent with a crucial role for IL-6, loss of the main regulator of this pathway, SOCS3, leads to a broadening of the population of genes responsive to LPS, suggesting that an overactivation of the IL-6/JAK/STAT3 pathway leads to an increased transcriptional response that could explain our prior findings of severe brain injury in these mice. To identify any potential sequelae of this acute response, we performed brain TRAP-seq following a battery of behavioral tests in mice after apparent recovery. We found that the transcriptional response returns to baseline within days post-challenge. Despite the transient nature of the response, we observed that mice that recovered from the endotoxemic shock showed mild, sex-dependent cognitive impairment, suggesting that the acute brain injury led to sustained, non-transcriptional effects. A better understanding of the transcriptional and non-transcriptional changes in response to shock is needed in order to prevent and/or revert the devastating consequences of septic shock.

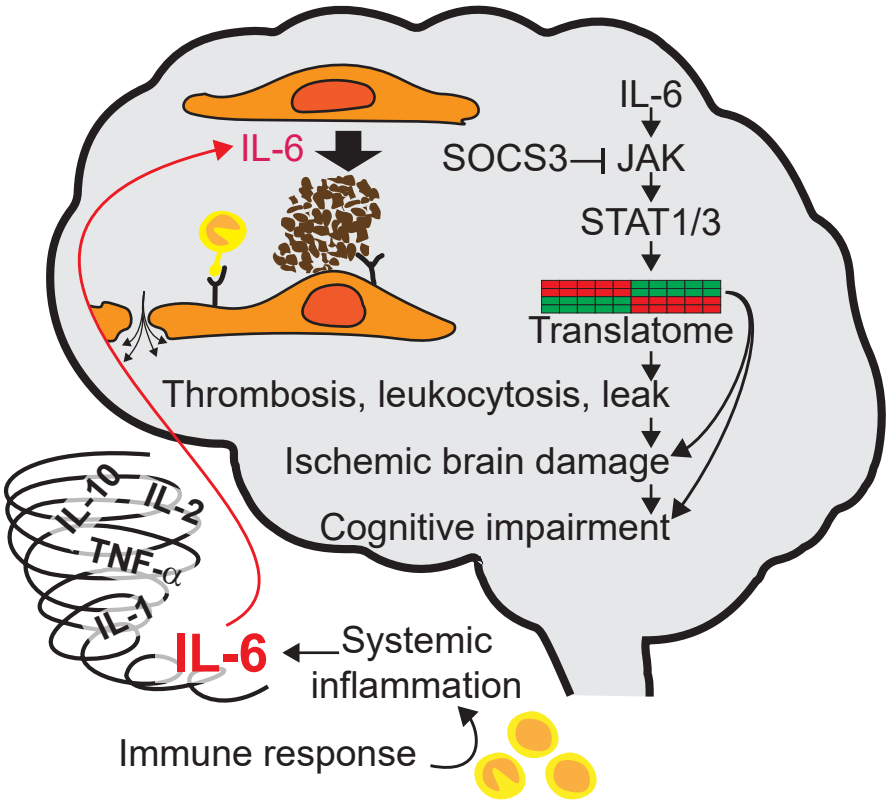
IL-6
IL-6
SOCS3
JAK
STAT1/3
Translatome
Thrombosis, leukocytosis, leak
Ischemic brain damage
Cognitive impairment
IL-10
IL-2
TNF-α
IL-1
IL-6
Systemic inflammation
Immune response

Introduction

Sepsis-associated encephalopathy (SAE) is a common manifestation in septic patients. It is characterized by diffuse cerebral dysfunction in the absence of a direct brain infection and often clinically manifests as delirium or coma (Fong TG et al., 2009;Gofton TE and Young GB, 2012;Hughes CG et al., 2016;Tokuda R et al., 2023). Acute encephalopathy occurs approximately in 70% of patients admitted at intensive care units (ICU) (Mazeraud A et al., 2020). Delirium usually resolves with the patient's overall improvement (Fong TG, et al., 2009). However, occurrence of SAE is associated with increased ICU stay, six-month mortality post-discharge, and higher risk of long-term cognitive impairment and dementia (Gofton TE and Young GB, 2012;Iwashyna TJ et al., 2010). The risks are higher in patients over 65 years old (Peterson JF et al., 2006) and those with more severe sepsis (Tokuda R, et al., 2023). Patients admitted at the ICU due to shock are at high risk of developing multiorgan failure, in large part due to a dysregulated inflammatory reaction that involves large concentrations of circulating cytokines, a condition usually known as a 'cytokine storm' (Tisoncik JR et al., 2012). The mechanisms driving encephalopathy are thought to involve an impaired microvascular blood-brain barrier, coagulopathy, and reduced perfusion, in response to systemic inflammatory cytokines (Crippa IA et al., 2023;Daneman R and Prat A, 2015;Gofton TE and Young GB, 2012;Hughes CG, et al., 2016;Peng X et al., 2021;Schramm P et al., 2012;Sweeney MD et al., 2019). Thus, targeting the brain microvasculature response to shock is a promising avenue to prevent or limit SAE. However, we do not fully understand the mechanisms by which the brain endothelium responds to severe systemic inflammatory signals that lead to brain microvascular dysfunction and SAE.

The role of interleukin-6 (IL-6) in systemic inflammatory conditions is well established (Hou T et al., 2015;Hunter CA and Jones SA, 2015;Remick DG et al., 2005). Prior work showed that IL-6 promotes a sustained loss of endothelial barrier function, both directly (Alsaffar H et al., 2018) and as part of an autocrine loop in response to LPS or TNF (Martino N et al., 2022). We previously reported that a single LPS injection led to increased brain vascular permeability 15 hours post-challenge (Martino N et al., 2021). Mice lacking endothelial expression of SOCS3 (SOCS3iEKO), the main negative regulator of the IL-6/JAK/STAT3 pathway, displayed significantly higher brain microvascular leak and organ injury than wild-type (WT) control mice (Martino N, et al., 2021), demonstrating a critical role for this pathway in the regulation of the blood-brain barrier in response to systemic inflammation.

The mechanisms driving LPS- and IL-6-induced brain endothelial dysfunction and its consequences, however, remain largely unknown. To begin addressing this mechanism, we sought to perform translating ribosome affinity purification (TRAP) (Zhou P et al., 2013) and RNA-sequencing (TRAP-seq) from the brain endothelium to determine the transcriptional changes after an acute challenge. To determine potential sequelae, we performed TRAP-seq following a battery of behavioral tests in mice after apparent recovery. We found that LPS induces a strong acute transcriptional response in the brain endothelium that returns to baseline within days post-challenge. Consistent with a critical role for the IL-6 pathway, SOCS3iEKO mice displayed an exacerbated transcriptional response. Despite the transient transcriptional changes, mice displayed mild, sex-specific cognitive impairment, suggesting lasting effects in brains exposed to a single endotoxemic shock.

Experimental Procedures

Materials, antibodies, and primers

The commercial sources for critical reagents and their catalog numbers are listed in Supplemental Table 1. Supplemental Table 2 lists all primers used.

Mice

All mouse experiments were approved by the Animal Resource Facility (ARF) at Albany Medical College and were performed in accordance with the Institutional Animal Care and Use Committee (IACUC)-approved protocols and followed MQTiPSS(Osuchowski MF et al., 2018) guidelines for randomization, masking, and euthanasia following standardized criteria.

Endothelial-specific TRAP mice generation was recently reported (Bossardi Ramos R et al., 2023). Briefly, B6.Tg(Cdh5-cre/ERT2)1Rha (Cdh5-CreERT2 endothelial driver) mice (Wang Y et al., 2010) were crossed with B6.129S4-Gt(ROSA)26Sortm1(CAG-EGFP/Rpl10a,-birA)Wtp/J (Rosa26fsTRAP) mice (Zhou P, et al., 2013) previously backcrossed to a C57Bl/6 background (a kind gift from Dr Patrick Murphy, University of Connecticut) and with B6;129S4-Socs3tm1Ayos/J (SOCS3$^{fl/fl}$ conditional knockout) (Yasukawa H et al., 2003) mice (The Jackson Laboratory). Tamoxifen-inducible endothelial-specific SOCS3 KO and WT littermate control mice for all experiments were generated by crossing two SOCS3$^{fl/+}$ heterozygote mice. All experimental mice carried homozygous Cre and GFP/Rpl10a transgenes. Genotypes and sex were confirmed with PCR genotyping (Supplemental Table 2). All mice received IP injections of 2mg/100µl tamoxifen for 5 consecutive days. All the experiments were performed 2 to 3 weeks after the end of tamoxifen injections. Mice were housed in pathogen-free rooms with controlled humidity and temperature, and 12 h light/dark cycles. A group of equal to or less than five mice lived in Allentown cages with accessible food and water ad libitum.

Acute systemic inflammation was induced by a single IP injection of 250µg LPS dissolved in 250µl of sterile saline solution. Control mice were injected with 250µl of sterile saline solution. Severity scores were assessed 13 hours after the LPS injection based on a scoring system as previously described (Bossardi Ramos R, et al., 2023;Martino N, et al., 2021). Immediately after, weight and temperature were measured. Mice were either euthanized 15 hours after the LPS injection, or scored (severity, temperature, weight) daily for four days. Behavioral tests as described below were performed between days five and eight. Following euthanasia, organs were collected for TRAP-seq.

TRAP-seq and bioinformatics

Endothelial RNA isolation was performed with modified established TRAP assay protocols (Heiman M et al., 2014;Zhou P, et al., 2013). Mice were euthanized with an overdose of pentobarbital. The chest cavity was opened immediately after confirmation of the absence of a paw reflex, and mice were subjected to an intracardiac perfusion with ice-cold HBSS containing 100 µg/ml CHX for 2 minutes at a rate of 5 ml/min. Brains were immediately removed and placed in plates containing 1 ml of dissection buffer and minced with razor blades pre-rinsed with RNAse Away solution. Approximately 200 mg of minced tissue was moved to RNAse-free tubes and lysed using RNAse-free disposable pestles. Samples were then centrifuged at 4 °C, 2000x g for 10 minutes. The supernatant was removed to a new tube and then 1/9 volume of 10% Igepal and 1/9 volume of 300 mM DHPC were added. Tubes were mixed by inversion several times and incubated for 5 minutes on ice. Then, samples were centrifuged at 4 °C 20,000x g for 10 minutes. 50 µl of the supernatant was transferred to a new tube for processing total RNA and the rest was transferred to another new tube for ribosome pulldown for endothelial-specific RNA. For total RNA, 500 µl of Trizol were added to each tube and RNA extraction was conducted with 100 µl of Chloroform. Then supernatant was moved to RNeasy Micro spin columns and an equal volume of 70% EtOH (approx. 350µl) was added to purify RNA by following the manufacturer's instructions. For the TRAP RNA, supernatants were incubated with prewashed Dynabeads on a nutating rocker for 15 minutes at RT to remove non-specific binding to the beads, and magnets were used for separation. The supernatant was then incubated with Dynabeads bound to anti-EGFP antibodies on a nutating rocker for 45 minutes at 4 °C. Followed by the washes with RNA buffer, the beads reached RT and then incubated for an extra 5 minutes in RLT buffer containing β-mercaptoethanol. RNA was then purified using RNeasy Micro spin columns following the manufacturer's instructions.

A total of 500 ng (whole brain) or 100 ng (brain TRAP) RNA from each brain was sent to Azenta Life Sciences for standard (bulk RNA-seq) or ultra-low RNA sequencing (TRAP-seq). Raw sequencing files were deposited in NCBI's Gene Expression Omnibus and are accessible through GEO Series accession number GSE253438. Mapping to the mouse genome (mm10) was performed in R/Bioconductor (Huber W et al., 2015) using the Rsubread (Liao Y et al., 2019) package. Differential gene expression was calculated using edgeR (Robinson MD et al., 2010) package. Gene Set Enrichment Analysis of Gene Ontology was performed using ClusterProfiler (Yu G et al., 2012) package. Upstream analysis (enrichment in pathways and transcription factors) of each datasets was performed using the DecoupleR (Badia IMP et al., 2022) package, the PROGENy model (Schubert M et al., 2018), and the CollecTRI network (Muller-Dott S et al., 2023).

Behavioral tests

Except for the nest building assay, mice were moved to a room with dim light for 1 h to acclimate to the surrounding. The maze and arena were cleaned with 70% ethanol between trials. After each test, mice were moved to a "recovery cage" to separate the mouse from all untested cage mates. Mouse performances were recorded with a camera placed above the behavioral maze or arena, and mouse movement was tracked and analyzed with ANY-maze software.

Y-maze: Mice were placed in a Y-shaped maze with 3 arms for 5min to freely explore the routes. Data was analyzed manually by counting the number of alternating entries to each of the three arms. The percent alternation index was calculated as [triad/(number of arm entries-2)]*100. Mice that jumped out of the maze were excluded.

Open field: Mice were placed individually in the arena (box 495 x495 mm) for 10 min. Mouse activities were recorded with the video camera on top of the box and mouse movements were tracked with ANY-maze software. A 4x4 grid was drawn over the video to track the animal's position over time. The percent center time index was obtained by dividing the time spent in the 4 center squares over the total experimental time.

Novel object recognition (NOR) test: Mice were placed individually in the same arena as for the open field test but containing two identical rubber ducks 8 cm from the wall in the northeast corner and northwest corner of the arena respectively. Training was performed by placing the mice for 10 minutes in the arena to familiarize the mice with these objects. Mice were then returned to their cages. After 1h, mice were returned to the arena for the test trial. At this time, the right rubber duck was replaced with a glass cup of a similar size. Mouse movements were tracked with ANY-maze software for 10 minutes. The time spent on each object was evaluated by determining the time spent within a 5 cm radius from the object. The recognition index was calculated as [(time with novel object / total time with objects)*100].

Nest building: Following the NOR test, mice were single-caged with two nestlets and allowed to freely make nests overnight (16 h). Mice were then removed back to their original group cages for later tissue collection. Nests were scored from 1-5 with 0.5 increments, according to a well-established scale (Deacon RM, 2006). Briefly, scores were: 1, >90% intact nestlet; 2, partially torn nestlet; 3, nestlet mostly shredded but often no identifiable nest site; 4, an identifiable but flat nest; 5, a near perfect nest. Scores from three independent scorers were averaged.

Cell culture

HCMEC/D3 were obtained from Millipore Sigma (catalog number SCC066). HBEC-5i cells were purchased from ATCC (catalog #CRL-3245) and maintained following manufacturer's instructions. HCMEC/D3 cells were cultured in EndoGRO-MV Complete Culture Media (Millipore Sigma). HBEC-5i cells were cultured in DMEM:F-12 1:1 mixture with L-glutamine and HEPES media (ATCC 30-2006TM)

containing 40g/mL endothelial growth supplement (ECGS) and 10% fetal bovine serum. To induce IL-6 signaling, cells were treated with a combination of 200 ng/mL recombinant human IL-6, 2 µg/mL LPS, or 10 ng/mL TNF in the presence or absence of 100 ng/mL sIL-6Rα (sIL6R). A similar amount of PBS was used for controls. HUVEC were isolated and grown as described previously (Bossardi Ramos R, et al., 2023;Martino N, et al., 2022;Martino N, et al., 2021).

RT-qPCR

After cell treatments, cells were lysed with Trizol and total RNA was isolated according to manufacturer's instructions. Primescript RT Master Mix was used to make cDNA from 400ng of total RNA following manufacturer's instructions. cDNA was diluted 10-fold in nuclease-free water. 2 µL of cDNA was used per PCR reaction. qPCR was performed in a StepOnePlus or a QuantStudio 3 (Applied Biosystems) instrument using SYBR green-based iTaq supermix (Bio-Rad) and 2 pmol primers (Thermo Fisher). Fold induction was calculated using the ΔΔCt method using GAPDH as housekeeping gene. Primer sequences utilized are listed in Supplemental Table 2.

Statistics

All statistical analysis and graphs were made in GraphPad Prism, version 6. Analysis for RNA expression levels was performed using a one-way ANOVA comparing all samples versus a control (designated in each figure). Analysis for behavioral tests was performed using a two-way ANOVA and Holm–Šídák post hoc tests comparing all samples versus a control group (designated in each figure). A two-tailed *P* value of less than 0.05 was considered significant.

Results

Systemic inflammation induces an acute proinflammatory brain microvascular transcriptional response

To study brain endothelial-specific transcriptional response to systemic inflammation, we crossed Rosa26 fsTRAP transgene with mice carrying a cdh5-CreERT2 inducible endothelial Cre driver. After tamoxifen treatment, mice were challenged with a single intraperitoneal bolus of LPS or vehicle (saline solution). Fifteen hours later, mice were euthanized and whole brains were processed for bulk RNA-seq (whole brain gene expression) and TRAP-seq (endothelial-specific translatome) (Figure 1A). A strong enrichment in endothelial-specific markers and a loss of non-endothelial gene expression demonstrate the efficiency and specificity of the TRAP protocol (Figure 1B). The TRAP-seq response is consistent with endothelial responses measured by single-cell RNA-seq in recent studies of aging and neuroinflammation (Allen WE et al., 2023;Jeong HW et al., 2022). We then compared our data with published brain TRAP from Tie2-Cre;Rpl22-HA mice (Cleuren ACA et al., 2019). Consistent with the increased specificity of the cdh5-CreERT2 (Payne S et al., 2018), we found that many genes induced by LPS in the Tie2-Cre-driven TRAP were not altered in the cdh5-CreERT2-driven TRAP data (Figure 1C). This is likely not due to differences in the LPS challenge, because the total brain RNA-seq demonstrated a strong correlation between the two datasets (Figure 1D).

As expected, gene set enrichment analysis of the endothelial transcriptional response to LPS demonstrates a strong activation of innate immunity and proinflammatory signaling (Figure 1E). This challenge induced strong neuroinflammation, as determined by increased expression of GFAP, TNF, and many other proinflammatory markers in whole brain (Supplemental Table 3). Although the transcriptional endothelial response to LPS showed a strong correlation with that of the whole brain (Figure 1F), multiple genes altered only in the TRAP-seq dataset suggested a marked endothelial-specific hypoxic response (Figure 1G).

We then compared the transcriptional response of SOCS3iEKO mice to littermate control mice. SOCS3 deletion on SOCS3iEKO mice was confirmed by the TRAP-seq data (Figure 2A). The highest responsive genes to LPS were only modestly affected by the loss of SOCS3 (Figure 2B), suggesting an already maximal response to this gene subset. However, SOCS3iEKO mice responded with a much wider transcriptional response to LPS (Figure 2C-D, Supplemental Table 4). Pathway and transcription factor enrichment analysis of the SOCS3iEKO response demonstrated a strong activation of the JAK/STAT pathway and other transcription factors we previously identified as regulated by IL-6 (Figure 2E-G). Consistent with a crucial role for IL-6 driving organ damage, the level of expression in the brain endothelium correlated with the disease severity scoring (Figure 2H).

The proinflammatory response quickly returns to baseline levels upon shock resolution

We then sought to determine if this acute LPS challenge led to behavioral deficits. We tracked the disease severity (Bossardi Ramos R, et al., 2023;Martino N, et al., 2021) for four days prior to a battery of behavioral tests and brain TRAP-seq (Figure 3A). We performed this assay only in WT mice, since SOCS3iEKO mice do not survive this LPS challenge (Martino N, et al., 2021). All mice had completely recovered by day 4 (Figure 3B). Brain TRAP-Seq and whole brain RNA-seq data from mice after recovery from LPS demonstrate the transient nature of the majority of the endothelial transcriptional responses (Figure 3C, Supplemental Table 5). However, a limited inflammatory response to LPS remains, with increased brain endothelial mRNA levels of several proinflammatory genes (Supplemental Table 5). Consistent with the transient nature of the inflammatory response, we detected limited, sex-dependent behavioral changes in recovering mice compared to saline-treated mice. We found that female mice treated with LPS performed poorly in the nest building test (Figure 3D), while LPS-treated males displayed deficits in the Y maze test (Figure 3E). Both males and females showed no changes in the novel object recognition and the open field tests (Figure 3F-G). No sex-dependent baseline differences were observed in saline-treated mice (Figure 3D-G).

Endothelial cells derived from a human brain show a transient transcriptional response to proinflammatory stimuli

We then performed in vitro assays to determine whether the transcriptional response observed in our TRAP data was a direct effect of LPS or IL-6 signaling on endothelial cells. An LPS challenge quickly induced IL6 expression in the immortalized microvascular brain endothelial cell line HCMEC/D3 (Figure 4A). This response was further increased if cells were challenged with LPS in the presence of the soluble form of the IL-6 receptor subunit gp80 (sIL-6Rα, denoted as LPS+R). Consistent with our previous observations in human primary endothelial cells(Martino N, et al., 2022), this co-stimulation allows for an increased transcriptional response, as evidenced by the increased SOCS3 expression. LPS+R also induced an increase in expression of multiple genes identified by our TRAP-seq (Figure 4A). This suggested an IL-6-dependent autocrine signal in response to LPS. To directly assess the effects of IL-6, we challenged these cells with a combination of IL-6 and its soluble receptor (IL-6+R). As expected, this challenge quickly induced an increase in IL6 and SOCS3 (Figure 4B). In support for a direct response to IL-6, the same challenge promoted a significant increase in the expression of CXCL10, NAMPT and CD47 (Figure 4B). We observed a similar response to LPS and IL-6 in cells originally derived from human brain cortex endothelium (HBEC-5i, Figure 5A-C). However, HCMED/D3 cells retain much stronger expression of endothelial markers than HBEC-5i cells (Figure 5D), suggesting that HBEC-5i cells lost many of its endothelial characteristics during cell culture. Notably, HCMEC/D3 demonstrated a mild but significant response to IL-6 in the absence of recombinant sIL-6Rα (Figure 4B). This is likely due to the increased endogenous sIL-6Rα expression in HCMEC/D3 cells compared to other endothelial cells (Figure 5E).

Discussion

The mechanisms driving sepsis encephalopathy are thought to involve an impaired microvascular blood brain barrier, hypo- and hyper-coagulation, and reduced perfusion in response to systemic inflammatory cytokines (Crippa IA, et al., 2023;Daneman R and Prat A, 2015;Gofton TE and Young GB, 2012;Hughes CG, et al., 2016;Peng X, et al., 2021;Schramm P, et al., 2012;Sweeney MD, et al., 2019). Post-mortem analysis of septic shock decedents shows a pathology consistent with severe brain endotheliopathy, including edema, hemorrhage, microthrombi, and ischemia that is associated with higher IL-6 expression, microglia activation and neuronal apoptosis (Barichello T et al., 2022;Heming N et al., 2017;Munster BC et al., 2011;Sharshar T et al., 2004). Consistent with this mechanism, multiple experimental studies in small (Martino N, et al., 2021;Rosengarten B et al., 2007) and large (Taccone FS et al., 2014;Taccone FS et al., 2010) animals demonstrate that shock leads to severe brain microvascular dysfunction. Here, we present evidence that an acute inflammatory reaction leads to a strong but transient transcriptional profile in the brain endothelium. While this response is strongly correlated with that of the whole brain, we identified a transcriptional subset that represents an endothelial-specific response. Notably, this subset suggested an acute brain hypoxic event in response to LPS. We had previously shown that this challenge leads to a disruption in the blood-brain barrier that is worsened in mice lacking endothelial expression of the IL-6 signaling pathway inhibitor SOCS3 (Martino N, et al., 2021). We show here that loss of SOCS3 leads to a broadening of the population of genes responsive to LPS, suggesting that an overactivation of the IL-6/JAK/STAT3 pathway leads to an increased transcriptional response that could explain the severe brain injury in these mice. Notably, in WT mice, this transcriptional response returns essentially to baseline levels only days after the shock. Despite the transient nature of the response, we observed that mice that recovered from the endotoxemic shock showed mild, sex-dependent cognitive impairment, suggesting that the acute brain injury led to sustained, non-transcriptional effects.

There is strong evidence that IL-6 is a causal factor in the development of cognitive impairment (Boots EA et al., 2022;Bradburn S et al., 2017;Lyra ESNM et al., 2021;Papassotiropoulos A et al., 1999;Rothaug M et al., 2016;Wright CB et al., 2006). Much less is known about the role of IL-6 in SAE and its sequelae. A recent systematic review demonstrates increased IL-6 expression in postmortem brains of septic patients when compared to non-septic decedents (Barichello T, et al., 2022). IL-6 was found to be increased in cerebrospinal fluid (but not in plasma) of patients with all-cause encephalitis (Wang X et al., 2022). In many animal models, systemic IL-6 signaling disrupts blood-brain barrier, promotes coagulopathy, and increases leukocyte infiltration (Kang SJ and Kishimoto T, 2021). In mice, brain IL-6 is associated with aging (Godbout JP and Johnson RW, 2004) and with endotoxin-induced neuroinflammation (Henry CJ et al., 2008). Consistent with a crucial role, blockade of circulating IL-6 signaling improved survival and cognitive functions in septic (Jiang SF et al., 2023) and trauma (Hu J et al., 2018) mouse models. The transcriptional data presented here is consistent with a critical role for IL-6 signaling acting directly on the brain endothelium. LPS induced a strong expression of multiple targets of the IL-6 pathway, including SOCS3 and IL-6 itself, that was observed in both whole brain and endothelial-specific RNA isolates. Mice lacking endothelial expression of SOCS3 displayed a stronger transcriptional response to LPS. Notably, IL-6 expression was undetectable in both WT and SOCS3iEKO saline groups, but SOCS3iEKO mice showed a 4-fold stronger response than WT mice in response to LPS. Bioinformatic analysis of the transcriptional response of SOCS3iEKO mice compared to WT mice confirmed the overactivation of the JAK/STAT3 signaling axis. Moreover, direct IL-6 stimulation of cultured brain endothelial cells induced an increase in expression of multiple proinflammatory genes identified by our TRAP-seq approach. How these changes may affect brain function in shock survivors, however, remains to be determined.

Little is known regarding sex- or gender-specific risks of developing post-intensive care cognitive decline and dementia. Some clinical studies found an association with sex or gender, while others did

not (Hiser SL et al., 2023;Lee M et al., 2020;Merdji H et al., 2023;Modra LJ et al., 2022;Neufeld KJ et al., 2020). Despite the endothelial and whole brain transcriptional profile returning to baseline levels after recovery from LPS, we identified mild, sex-dependent behavioral changes remaining well beyond severity scoring and temperature returned to normal levels. These findings are consistent with sex-specific cognitive deficits in mouse models of brain hypoperfusion (Gannon OJ et al., 2022;Robison LS et al., 2020;Salinero AE et al., 2020). It is not yet known however if similar processes drive cognitive decline in these two models. Future work is required to dissect the mechanisms driving this sex-specific response.

Legends to figures

Figure 1. Transcriptional response to LPS in the brain endothelium. (A) Schematic of TRAP approach. (B) Ratio of TRAP-seq over whole brain RNA-seq normalized counts obtained from the same brains. (C) Scatter plots to illustrate the extent of correlation between the brain endothelial responses to LPS as measured in this manuscript (Lu) or by a Tie2-Cre driver (Cleuren ACA, et al., 2019). The red ellipse denotes the gene set responsive in tie2-Cre+ cells but not in cdh5-CreERT2+ mice. (D) Same as in C, but data reflects bulk brain RNA-Seq demonstrating strong identity between the two datasets. (E) Top 20 entries (by normalized enrichment score, NES) of the gene set enrichment analysis of the endothelial transcriptional response to LPS. Shown at the right of each category are the number of enriched genes in the dataset and the total number of genes for each category. (F) Plot showing the correlation between the LPS response (log2 fold change) in whole brain vs brain TRAP. (G) Upstream pathway analysis of the endothelial-specific response, defined as the gene set that is significantly altered by LPS (fold change <0.5 or > 2, adj. p value < 0.05) in the brain TRAP-seq dataset but not in the whole brain bulk RNA-seq dataset.

Figure 2. Transcriptional dependence on the IL-6/STAT3/SOCS3 signaling axis. (A) Normalized counts for SOCS3 in brain TRAP and whole brain datasets from saline-treated mice. (B) Heatmap of the 100 most significantly changed genes in the brain endothelium (left) and the corresponding changes in the whole brain (right) of WT and SOCS3iEKO mice. Genes in gray were not detected by whole brain RNA-seq. (C) Volcano plot of the differential expression in response to LPS for either WT or SOCS3iEKO mice. (D) Venn diagram describing the number of differentially expressed genes in response to LPS (right). (E) Upstream pathway analysis of this dataset demonstrating the overactivation of JAK/STAT signaling. (F) Transcription factor enrichment confirming STAT1/3 activity. (G) Volcano plot of log10 p value vs log2 fold change (LPS-treated SOCS3iEKO vs WT mice) for all STAT3-dependent genes (as determined by DecoupleR/CollecTRI). (H) Correlation of endothelial levels of IL-6 gene expression vs severity score.

Figure 3. Sustained cognitive impairment despite transitory transcriptional changes. (A) Diagram of the experimental timeline. (B) Daily severity score after saline or LPS injection. Two-way ANOVA of repeated measurements. (C) Heatmap of the top 100 most significantly changed genes 15 hours post saline or LPS injection (left) and the corresponding genes 8 days after saline or LPS injection (right). (D-G) Behavioral tests following recovery from LPS. Assays for nest building (D), Y-maze (E), novel object recognition (F) and open field (G) were performed according to the timeline shown in A. Mann Whitney test (n=7—10 per group). Asterisks, $p < 0.05$.

Figure 4. Direct transcriptional regulation by LPS and IL-6 in cultured HCMEC/D3 cells. (A) Confluent HCMEC/D3 cells were treated for two or six hours PBS, PBS+ sIL-6Rα, LPS, or LPS+sIL-6Rα (LPS+R). RT-qPCR was performed to detect gene expression levels. (B) Confluent HCMEC/D3 cells were treated for two or six hours PBS, PBS+ sIL-6Rα, IL-6, or IL-6+sIL-6Rα (IL-6+R). RT-qPCR was performed to detect gene expression levels. Asterisks, $p < 0.05$ (Two-way ANOVA with Sidak post-hoc test against PBS control). Data compiled from three independent experiments performed in duplicate each.

Figure 5. Transcriptional regulation by LPS and IL-6 in cultured HBEC-5i cells. (A) Confluent HBEC-5i cells were treated for two hours with LPS, LPS+sIL-6Rα, or PBS. RT-qPCR was performed to detect IL6 or SOCS3 mRNA levels. Two-way ANOVA with Sidak post-hoc test. (B) HBEC-5i cells were treated with IL-6+R for two or six hours (or six hours of sIL-6Rα alone as control) prior to RT-qPCR to detect IL6 or SOCS3. One-way ANOVA with Sidak post-hoc test. (C) RNA from cells treated as in (B) was used to measure CXCL2, CXCL10, ICAM1, and NAMPT mRNA levels. Asterisks, $p < 0.05$ (Two-way ANOVA with Sidak post-hoc test). Data compiled from three independent experiments performed in duplicate each. (D) RT-qPCR using RNA obtained from confluent HCMEC/D3 and HBEC-5i cells to probe for expression of the endothelial markers PECAM, VWF, CDH5 and CLDN5. Primary human umbilical vein endothelial cells (HUVEC) were used as positive control. Shown are ΔCt values calculated as Ct for each gene of interest minus the Ct for the housekeeping gene GAPDH. (E) RT-qPCR from cells as above to probe for expression of IL-6Rα. Asterisks, $p < 0.05$ (One-way ANOVA with Tukey post-hoc test). Data compiled from three independent experiments performed in duplicate each.

Acknowledgements

This work was supported in part by grants R01GM124133, R01GM124133-S4 and ALZ-D-NTF 968957(APA), American Heart Association pre-doctoral award 916096 (SL), American Heart Association pre-doctoral award 908878 (AES), NINDS/NIA R01NS110749 (KLZ), and NIA U01AG072464 (KLZ).

References

Allen WE, Blosser TR, Sullivan ZA, Dulac C, Zhuang X (2023), Molecular and spatial signatures of mouse brain aging at single-cell resolution. Cell 186:194-208 e118.
Alsaffar H, Martino N, Garrett JP, Adam AP (2018), Interleukin-6 promotes a sustained loss of endothelial barrier function via Janus kinase-mediated STAT3 phosphorylation and de novo protein synthesis. American journal of physiology Cell physiology 314:C589-C602.
Badia IMP, Velez Santiago J, Braunger J, Geiss C, Dimitrov D, Muller-Dott S, Taus P, Dugourd A, et al. (2022), decoupleR: ensemble of computational methods to infer biological activities from omics data. Bioinform Adv 2:vbac016.
Barichello T, Generoso JS, Dominguini D, Corneo E, Giridharan VV, Sahrapour TA, Simoes LR, da Rosa MI, et al. (2022), Postmortem Evidence of Brain Inflammatory Markers and Injury in Septic Patients: A Systematic Review. Critical care medicine 50:E241-E252.
Boots EA, Feinstein DL, Leurgans S, Aiken-Morgan AT, Fleischman DA, Lamar M, Barnes LL (2022), Acute versus chronic inflammatory markers and cognition in older black adults: Results from the Minority Aging Research Study. Brain, behavior, and immunity 103:163-170.
Bossardi Ramos R, Martino N, Chuy D, Lu S, Zuo MXG, Balasubramanian U, Di John Portela I, Vincent PA, et al. (2023), Shock drives a STAT3 and JunB-mediated coordinated transcriptional and DNA methylation response in the endothelium. Journal of cell science.
Bradburn S, Sarginson J, Murgatroyd CA (2017), Association of Peripheral Interleukin-6 with Global Cognitive Decline in Non-demented Adults: A Meta-Analysis of Prospective Studies. Front Aging Neurosci 9:438.
Cleuren ACA, van der Ent MA, Jiang H, Hunker KL, Yee A, Siemieniak DR, Molema G, Aird WC, et al. (2019), The in vivo endothelial cell translatome is highly heterogeneous across vascular beds. Proceedings of the National Academy of Sciences of the United States of America 116:23618-23624.
Crippa IA, Vincent JL, Cavicchi FZ, Pozzebon S, Gaspard N, Maenhout C, Creteur J, Taccone FS (2023), Estimated Cerebral Perfusion Pressure and Intracranial Pressure in Septic Patients. Neurocritical Care.
Daneman R, Prat A (2015), The blood-brain barrier. Cold Spring Harb Perspect Biol 7:a020412.
Deacon RM (2006), Assessing nest building in mice. Nat Protoc 1:1117-1119.

Fong TG, Tulebaev SR, Inouye SK (2009), Delirium in elderly adults: diagnosis, prevention and treatment. Nature Reviews Neurology 5:210-220.
Gannon OJ, Robison LS, Salinero AE, Abi-Ghanem C, Mansour FM, Kelly RD, Tyagi A, Brawley RR, et al. (2022), High-fat diet exacerbates cognitive decline in mouse models of Alzheimer's disease and mixed dementia in a sex-dependent manner. J Neuroinflammation 19:110.
Godbout JP, Johnson RW (2004), Interleukin-6 in the aging brain. Journal of neuroimmunology 147:141-144.
Gofton TE, Young GB (2012), Sepsis-associated encephalopathy. Nat Rev Neurol 8:557-566.
Heiman M, Kulicke R, Fenster RJ, Greengard P, Heintz N (2014), Cell type-specific mRNA purification by translating ribosome affinity purification (TRAP). Nature protocols 9:1282-1291.
Heming N, Mazeraud A, Verdonk F, Bozza FA, Chretien F, Sharshar T (2017), Neuroanatomy of sepsis-associated encephalopathy. Critical care 21.
Henry CJ, Huang Y, Wynne A, Hanke M, Himler J, Bailey MT, Sheridan JF, Godbout JP (2008), Minocycline attenuates lipopolysaccharide (LPS)-induced neuroinflammation, sickness behavior, and anhedonia. J Neuroinflammation 5:15.
Hiser SL, Fatima A, Ali M, Needham DM (2023), Post-intensive care syndrome (PICS): recent updates. J Intensive Care 11:23.
Hou T, Huang D, Zeng R, Ye Z, Zhang Y (2015), Accuracy of serum interleukin (IL)-6 in sepsis diagnosis: a systematic review and meta-analysis. Int J Clin Exp Med 8:15238-15245.
Hu J, Feng X, Valdearcos M, Lutrin D, Uchida Y, Koliwad SK, Maze M (2018), Interleukin-6 is both necessary and sufficient to produce perioperative neurocognitive disorder in mice. British journal of anaesthesia 120:537-545.
Huber W, Carey VJ, Gentleman R, Anders S, Carlson M, Carvalho BS, Bravo HC, Davis S, et al. (2015), Orchestrating high-throughput genomic analysis with Bioconductor. Nature methods 12:115-121.
Hughes CG, Pandharipande PP, Thompson JL, Chandrasekhar R, Ware LB, Ely EW, Girard TD (2016), Endothelial Activation and Blood-Brain Barrier Injury as Risk Factors for Delirium in Critically Ill Patients. Critical care medicine 44:E809-E817.
Hunter CA, Jones SA (2015), IL-6 as a keystone cytokine in health and disease. Nature immunology 16:448-457.
Iwashyna TJ, Ely EW, Smith DM, Langa KM (2010), Long-term Cognitive Impairment and Functional Disability Among Survivors of Severe Sepsis. JAMA-J Am Med Assoc 304:1787-1794.
Jeong HW, Dieguez-Hurtado R, Arf H, Song J, Park H, Kruse K, Sorokin L, Adams RH (2022), Single-cell transcriptomics reveals functionally specialized vascular endothelium in brain. Elife 11.
Jiang SF, Shi DD, Bai L, Niu TF, Kang RT, Liu Y (2023), Inhibition of interleukin-6 trans-signaling improves survival and prevents cognitive impairment in a mouse model of sepsis. International immunopharmacology 119.
Kang SJ, Kishimoto T (2021), Interplay between interleukin-6 signaling and the vascular endothelium in cytokine storms. Experimental and Molecular Medicine 53:1116-1123.
Lee M, Kang J, Jeong YJ (2020), Risk factors for post-intensive care syndrome: A systematic review and meta-analysis. Aust Crit Care 33:287-294.
Liao Y, Smyth GK, Shi W (2019), The R package Rsubread is easier, faster, cheaper and better for alignment and quantification of RNA sequencing reads. Nucleic acids research 47:e47.
Lyra ESNM, Goncalves RA, Pascoal TA, Lima-Filho RAS, Resende EPF, Vieira ELM, Teixeira AL, de Souza LC, et al. (2021), Pro-inflammatory interleukin-6 signaling links cognitive impairments and peripheral metabolic alterations in Alzheimer's disease. Transl Psychiatry 11:251.
Martino N, Bossardi Ramos R, Chuy D, Tomaszek L, Adam AP (2022), SOCS3 limits TNF and endotoxin-induced endothelial dysfunction by blocking a required autocrine interleukin 6 signal in human endothelial cells. American journal of physiology Cell physiology.

Martino N, Ramos RB, Lu S, Leyden K, Tomaszek L, Sadhu S, Fredman G, Jaitovich A, et al. (2021), Endothelial SOCS3 maintains homeostasis and promotes survival in endotoxemic mice. JCI Insight 6.
Mazeraud A, Righy C, Bouchereau E, Benghanem S, Bozza FA, Sharshar T (2020), Septic-Associated Encephalopathy: a Comprehensive Review. Neurotherapeutics 17:392-403.
Merdji H, Long MT, Ostermann M, Herridge M, Myatra SN, De Rosa S, Metaxa V, Kotfis K, et al. (2023), Sex and gender differences in intensive care medicine. Intensive care medicine 49:1155-1167.
Modra LJ, Higgins AM, Pilcher DV, Bailey MJ, Bellomo R (2022), Sex Differences in Mortality of ICU Patients According to Diagnosis-related Sex Balance. American journal of respiratory and critical care medicine 206:1353-1360.
Muller-Dott S, Tsirvouli E, Vazquez M, Ramirez Flores RO, Badia IMP, Fallegger R, Turei D, Laegreid A, et al. (2023), Expanding the coverage of regulons from high-confidence prior knowledge for accurate estimation of transcription factor activities. Nucleic acids research 51:10934-10949.
Munster BC, Aronica E, Zwinderman AH, Eikelenboom P, Cunningham C, Rooij SE (2011), Neuroinflammation in delirium: a postmortem case-control study. Rejuvenation Res 14:615-622.
Neufeld KJ, Leoutsakos JS, Yan H, Lin S, Zabinski JS, Dinglas VD, Hosey MM, Parker AM, et al. (2020), Fatigue Symptoms During the First Year Following ARDS. Chest 158:999-1007.
Osuchowski MF, Ayala A, Bahrami S, Bauer M, Boros M, Cavaillon JM, Chaudry IH, Coopersmith CM, et al. (2018), Minimum quality threshold in pre-clinical sepsis studies (MQTiPSS): an international expert consensus initiative for improvement of animal modeling in sepsis. Intensive Care Med Exp 6:26.
Papassotiropoulos A, Bagli M, Jessen F, Bayer TA, Maier W, Rao ML, Heun R (1999), A genetic variation of the inflammatory cytokine interleukin-6 delays the initial onset and reduces the risk for sporadic Alzheimer's disease. Annals of neurology 45:666-668.
Payne S, De Val S, Neal A (2018), Endothelial-Specific Cre Mouse Models. Arteriosclerosis, thrombosis, and vascular biology 38:2550-2561.
Peng X, Luo Z, He S, Zhang L, Li Y (2021), Blood-Brain Barrier Disruption by Lipopolysaccharide and Sepsis-Associated Encephalopathy. Front Cell Infect Microbiol 11:768108.
Peterson JF, Pun BT, Dittus RS, Thomason JW, Jackson JC, Shintani AK, Ely EW (2006), Delirium and its motoric subtypes: a study of 614 critically ill patients. J Am Geriatr Soc 54:479-484.
Remick DG, Bolgos G, Copeland S, Siddiqui J (2005), Role of interleukin-6 in mortality from and physiologic response to sepsis. Infect Immun 73:2751-2757.
Robinson MD, McCarthy DJ, Smyth GK (2010), edgeR: a Bioconductor package for differential expression analysis of digital gene expression data. Bioinformatics 26:139-140.
Robison LS, Gannon OJ, Thomas MA, Salinero AE, Abi-Ghanem C, Poitelon Y, Belin S, Zuloaga KL (2020), Role of sex and high-fat diet in metabolic and hypothalamic disturbances in the 3xTg-AD mouse model of Alzheimer's disease. J Neuroinflammation 17:285.
Rosengarten B, Hecht M, Auch D, Ghofrani HA, Schermuly RT, Grimminger F, Kaps M (2007), Microcirculatory dysfunction in the brain precedes changes in evoked potentials in endotoxin-induced sepsis syndrome in rats. Cerebrovascular Diseases 23:140-147.
Rothaug M, Becker-Pauly C, Rose-John S (2016), The role of interleukin-6 signaling in nervous tissue. Biochimica et biophysica acta 1863:1218-1227.
Salinero AE, Robison LS, Gannon OJ, Riccio D, Mansour F, Abi-Ghanem C, Zuloaga KL (2020), Sex-specific effects of high-fat diet on cognitive impairment in a mouse model of VCID. FASEB J 34:15108-15122.
Schramm P, Klein KU, Falkenberg L, Berres M, Closhen D, Werhahn KJ, David M, Werner C, et al. (2012), Impaired cerebrovascular autoregulation in patients with severe sepsis and sepsis-associated delirium. Critical care 16.
Schubert M, Klinger B, Klunemann M, Sieber A, Uhlitz F, Sauer S, Garnett MJ, Bluthgen N, et al. (2018), Perturbation-response genes reveal signaling footprints in cancer gene expression. Nature communications 9:20.

Sharshar T, Annane D, de la Grandmaison GL, Brouland JP, Hopkinson NS, Francoise G (2004), The neuropathology of septic shock. Brain Pathol 14:21-33.
Sweeney MD, Zhao Z, Montagne A, Nelson AR, Zlokovic BV (2019), Blood-Brain Barrier: From Physiology to Disease and Back. Physiological reviews 99:21-78.
Taccone FS, Su FH, De Deyne C, Abdellhai A, Pierrakos C, He XR, Donadello K, Dewitte O, et al. (2014), Sepsis Is Associated With Altered Cerebral Microcirculation and Tissue Hypoxia in Experimental Peritonitis. Critical care medicine 42:E114-E122.
Taccone FS, Su FH, Pierrakos C, He XR, James S, Dewitte O, Vincent JL, De Backer D (2010), Cerebral microcirculation is impaired during sepsis: an experimental study. Critical care 14.
Tisoncik JR, Korth MJ, Simmons CP, Farrar J, Martin TR, Katze MG (2012), Into the eye of the cytokine storm. Microbiol Mol Biol Rev 76:16-32.
Tokuda R, Nakamura K, Takatani Y, Tanaka C, Kondo Y, Ohbe H, Kamijo H, Otake K, et al. (2023), Sepsis-Associated Delirium: A Narrative Review. Journal of Clinical Medicine 12.
Wang X, Delle C, Asiminas A, Akther S, Vittani M, Brøgger P, Kusk P, Vo CT, et al. (2022), Liver-secreted fluorescent blood plasma markers enable chronic imaging of the microcirculation. Cell Rep Methods 2:100302.
Wang Y, Nakayama M, Pitulescu ME, Schmidt TS, Bochenek ML, Sakakibara A, Adams S, Davy A, et al. (2010), Ephrin-B2 controls VEGF-induced angiogenesis and lymphangiogenesis. Nature 465:483-486.
Wright CB, Sacco RL, Rundek T, Delman J, Rabbani L, Elkind M (2006), Interleukin-6 is associated with cognitive function: the Northern Manhattan Study. J Stroke Cerebrovasc Dis 15:34-38.
Yasukawa H, Ohishi M, Mori H, Murakami M, Chinen T, Aki D, Hanada T, Takeda K, et al. (2003), IL-6 induces an anti-inflammatory response in the absence of SOCS3 in macrophages. Nature immunology 4:551-556.
Yu G, Wang LG, Han Y, He QY (2012), clusterProfiler: an R package for comparing biological themes among gene clusters. OMICS 16:284-287.
Zhou P, Zhang Y, Ma Q, Gu F, Day DS, He A, Zhou B, Li J, et al. (2013), Interrogating translational efficiency and lineage-specific transcriptomes using ribosome affinity purification. Proceedings of the National Academy of Sciences of the United States of America 110:15395-15400.

Figure 1

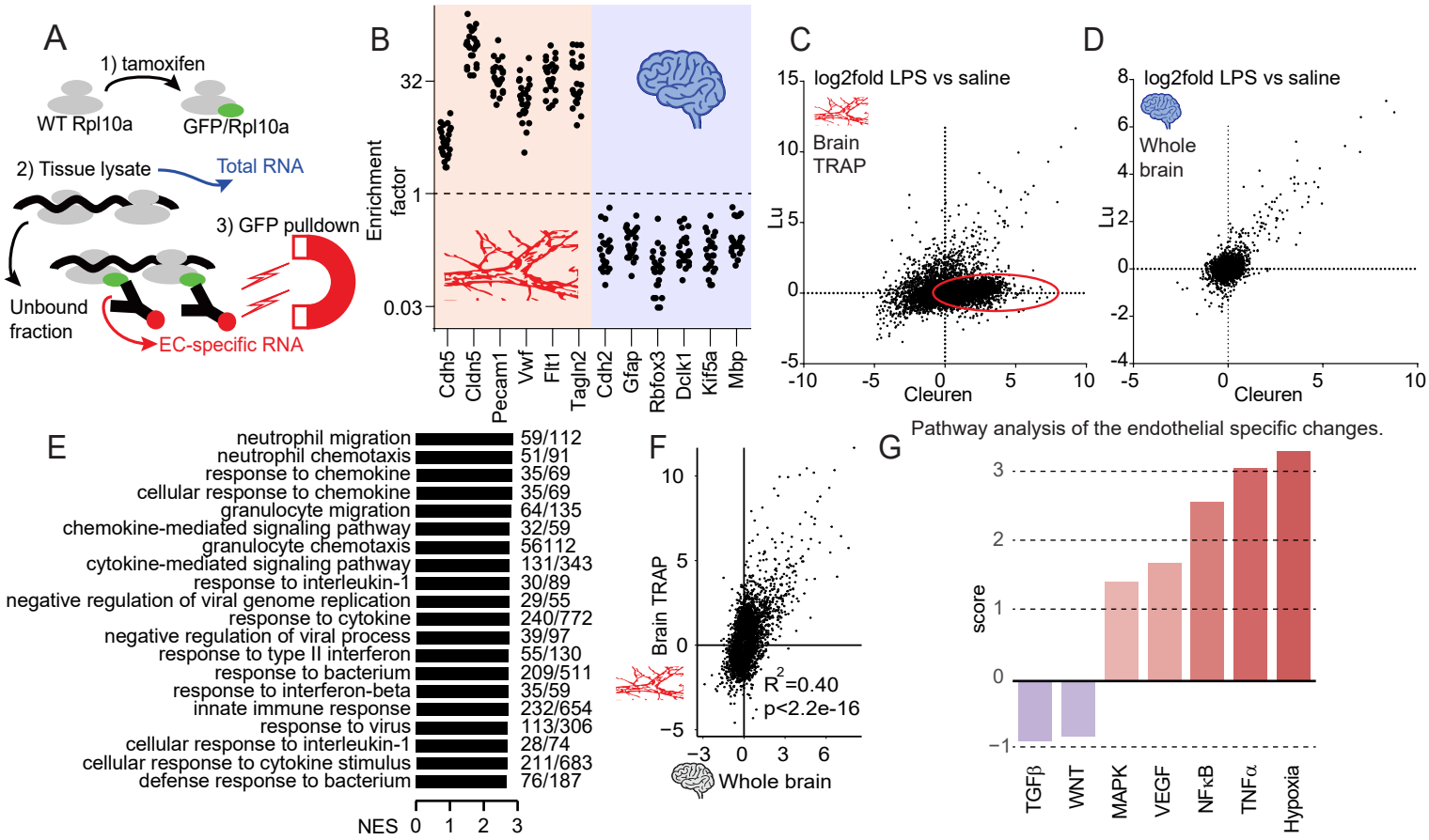

Figure 1. Transcriptional response to LPS in the brain endothelium. (A) Schematic of TRAP approach. (B) Ratio of TRAP-seq over whole brain RNA-seq normalized counts obtained from the same brains. (C) Scatter plots to illustrate the extent of correlation between the brain endothelial responses to LPS as measured in this manuscript (Lu) or by a Tie2-Cre driver (Cleuren ACA, et al., 2019). The red ellipse denotes the gene set responsive in tie2-Cre+ cells but not in cdh5-CreERT2+ mice. (D) Same as in C, but data reflects bulk brain RNA-Seq demonstrating strong identity between the two datasets. (E) Top 20 entries (by normalized enrichment score, NES) of the gene set enrichment analysis of the endothelial transcriptional response to LPS. Shown at the right of each category are the number of enriched genes in the dataset and the total number of genes for each category. (F) Plot showing the correlation between the LPS response (log2 fold change) in whole brain vs brain TRAP. (G) Upstream pathway analysis of the endothelial-specific response, defined as the gene set that is significantly altered by LPS (fold change <0.5 or > 2, adj. p value < 0.05) in the brain TRAP-seq dataset but not in the whole brain bulk RNA-seq dataset.

Figure 2

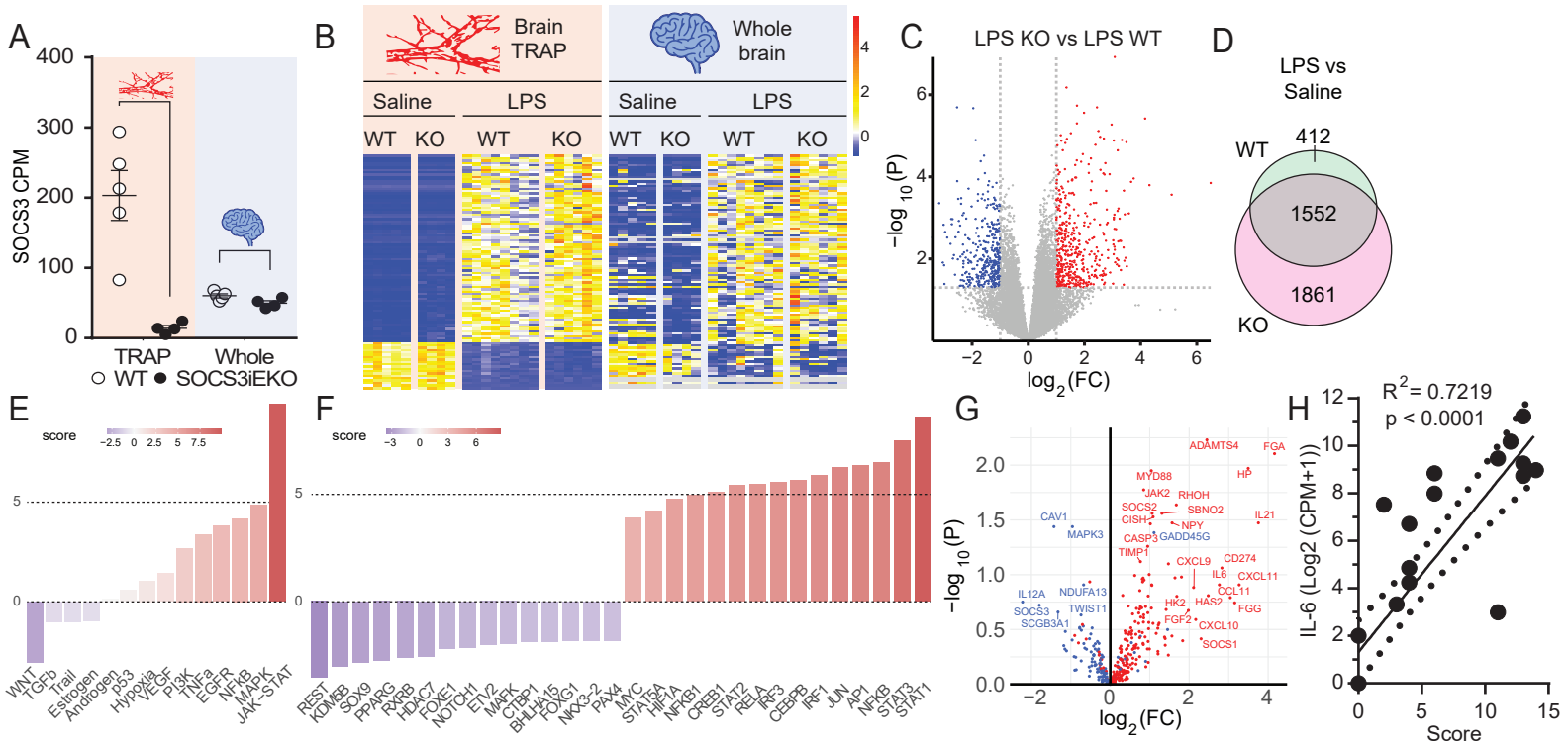

Figure 2. Transcriptional dependence on the IL-6/STAT3/SOCS3 signaling axis. (A) Normalized counts for SOCS3 in brain TRAP and whole brain datasets from saline-treated mice. (B) Heatmap of the 100 most significantly changed genes in the brain endothelium (left) and the corresponding changes in the whole brain (right) of WT and SOCS3iEKO mice. Genes in gray were not detected by whole brain RNA-seq. (C) Volcano plot of the differential expression in response to LPS for either WT or SOCS3iEKO mice. (D) Venn diagram describing the number of differentially expressed genes in response to LPS (right). (E) Upstream pathway analysis of this dataset demonstrating the overactivation of JAK/STAT signaling. (F) Transcription factor enrichment confirming STAT1/3 activity. (G) Volcano plot of log10 p value vs log2 fold change (LPS-treated SOCS3iEKO vs WT mice) for all STAT3-dependent genes (as determined by DecoupleR/CollecTRI). (H) Correlation of endothelial levels of IL-6 gene expression vs severity score.

Figure 3

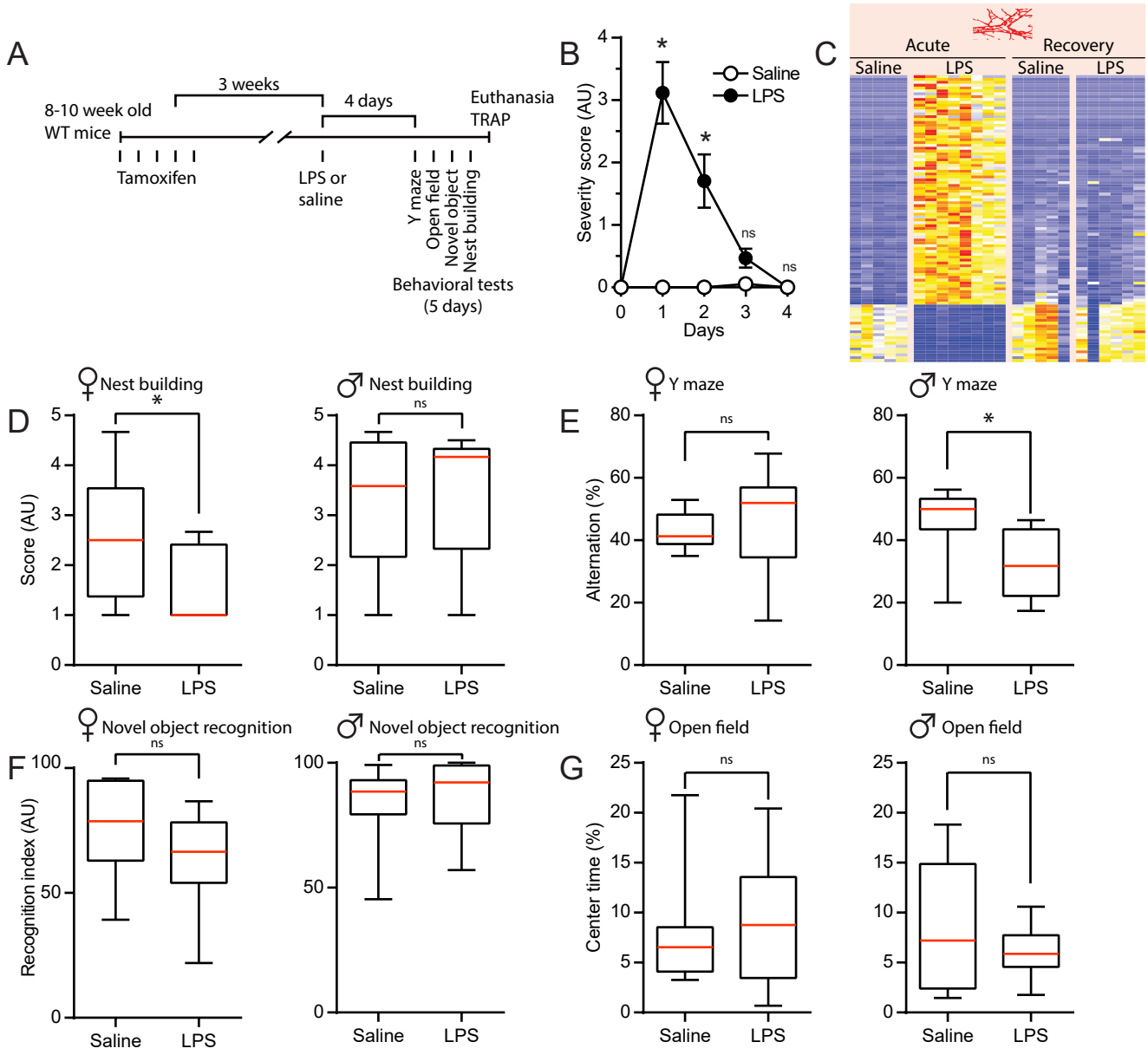

Figure 3. Sustained cognitive impairment despite transitory transcriptional changes. (A) Diagram of the experimental timeline. (B) Daily severity score after saline or LPS injection. Two-way ANOVA of repeated measurements. (C) Heatmap of the top 100 most significantly changed genes 15 hours post saline or LPS injection (left) and the corresponding genes 8 days after saline or LPS injection (right). (D-G) Behavioral tests following recovery from LPS. Assays for nest building (D), Y-maze (E), novel object recognition (F) and open field (G) were performed according to the timeline shown in A. Mann Whitney test (n=7—10 per group). Asterisks, $p < 0.05$.

Figure 4

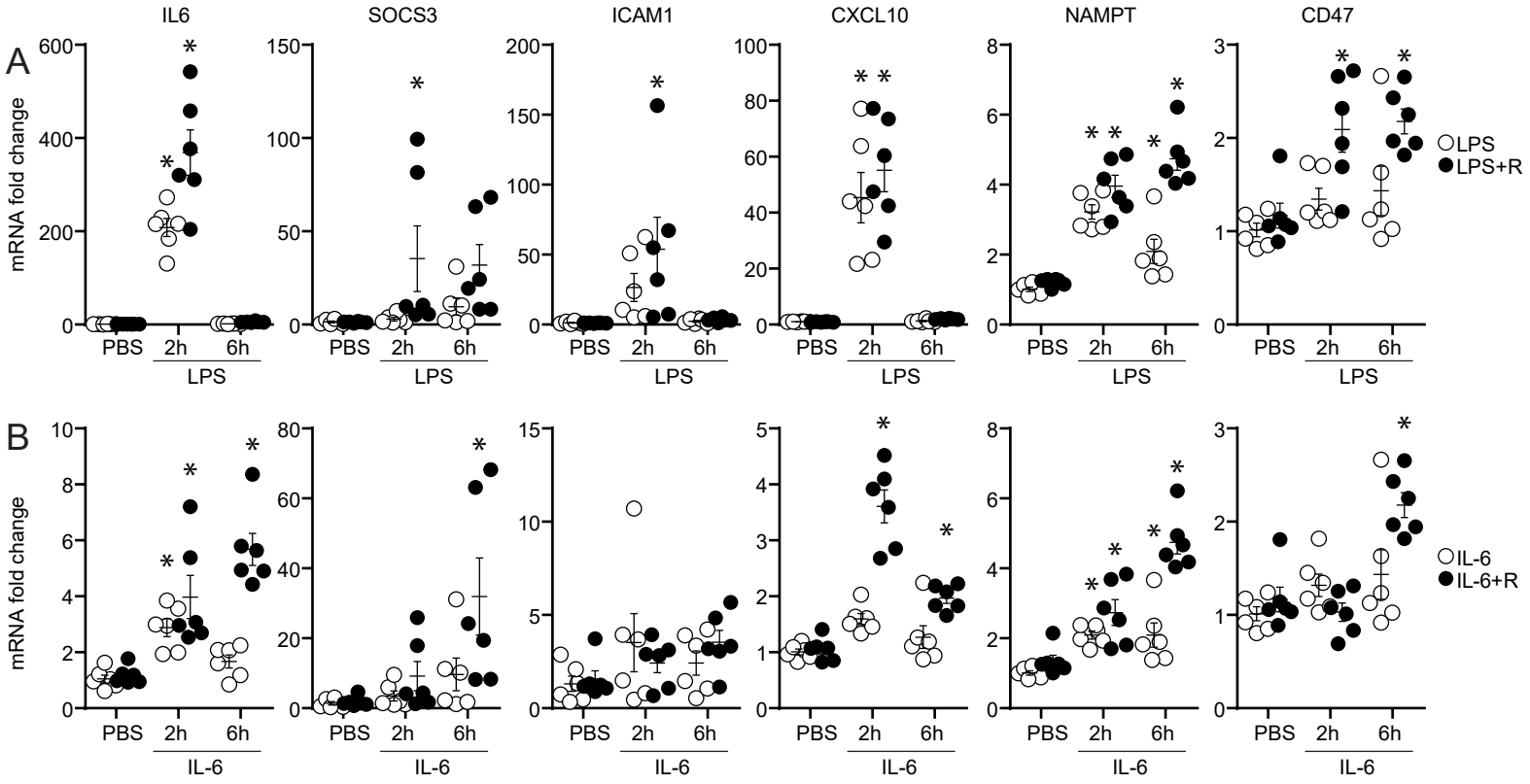

Figure 4. Direct transcriptional regulation by LPS and IL-6 in cultured HCMEC/D3 cells. (A) Confluent HCMEC/D3 cells were treated for two or six hours PBS, PBS+ sIL-6Rα, LPS, or LPS+sIL-6Rα (LPS+R). RT-qPCR was performed to detect gene expression levels. (B) Confluent HCMEC/D3 cells were treated for two or six hours PBS, PBS+ sIL-6Rα, IL-6, or IL-6+sIL-6Rα (IL-6+R). RT-qPCR was performed to detect gene expression levels. Asterisks, $p < 0.05$ (Two-way ANOVA with Sidak post-hoc test against PBS control). Data compiled from three independent experiments performed in duplicate each.

Figure 5

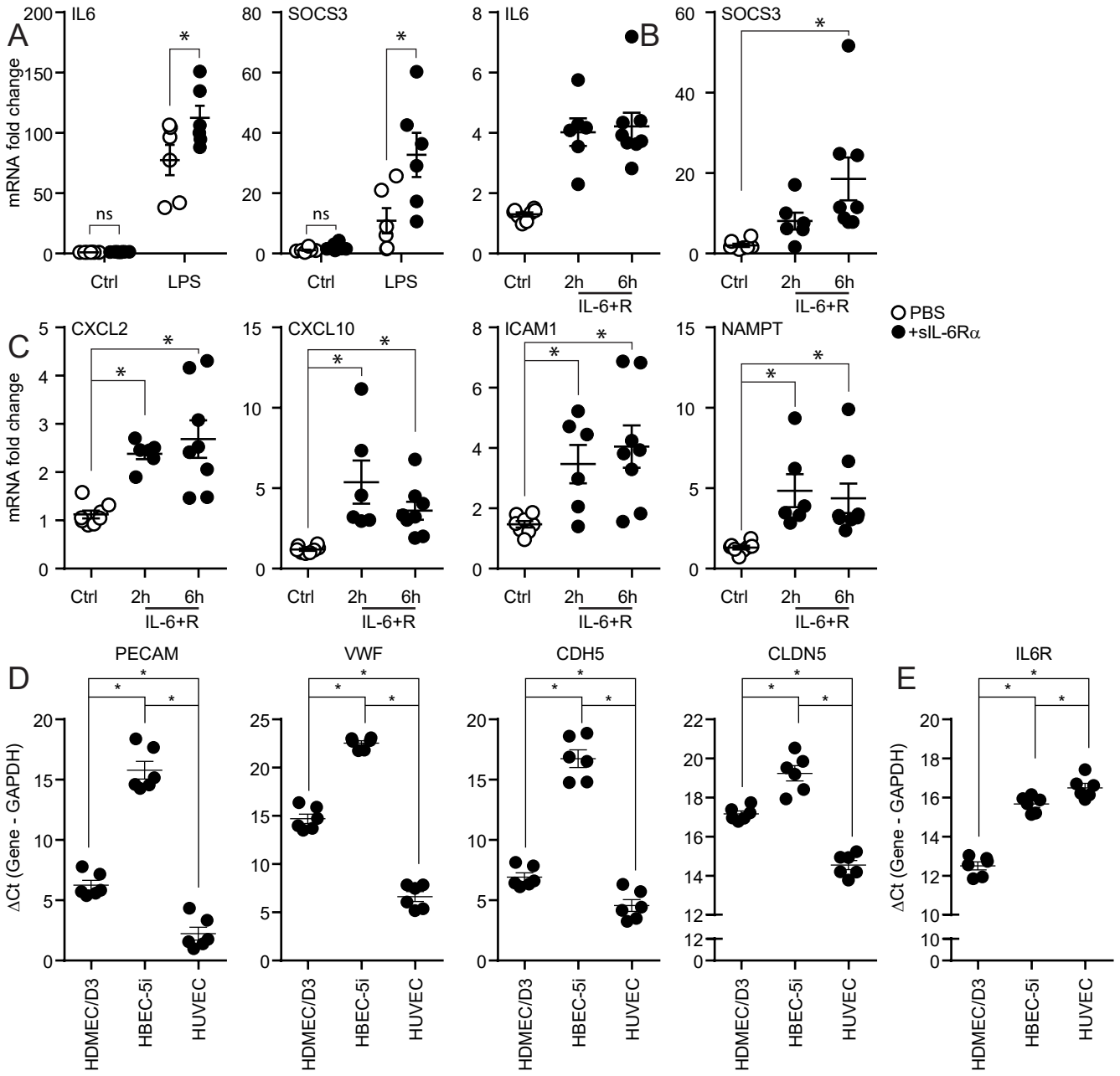

Figure 5. Transcriptional regulation by LPS and IL-6 in cultured HBEC-5i cells. (A) Confluent HBEC-5i cells were treated for two hours with LPS, LPS+sIL-6Rα, or PBS. RT-qPCR was performed to detect IL6 or SOCS3 mRNA levels. Two-way ANOVA with Sidak post-hoc test. (B) HBEC-5i cells were treated with IL-6+R for two or six hours (or six hours of sIL-6Rα alone as control) prior to RT-qPCR to detect IL6 or SOCS3. One-way ANOVA with Sidak post-hoc test. (C) RNA from cells treated as in (B) was used to measure CXCL2, CXCL10, ICAM1, and NAMPT mRNA levels. Asterisks, $p < 0.05$ (Two-way ANOVA with Sidak post-hoc test). Data compiled from three independent experiments performed in duplicate each. (D) RT-qPCR using RNA obtained from confluent HCMEC/D3 and HBEC-5i cells to probe for expression of the endothelial markers PECAM, VWF, CDH5 and CLDN5. Primary human umbilical vein endothelial cells (HUVEC) were used as positive control. Shown are ΔCt values calculated as Ct for each gene of interest minus the Ct for the housekeeping gene GAPDH. (E) RT-qPCR from cells as above to probe for expression of IL-6Rα. Asterisks, $p < 0.05$ (One-way ANOVA with Tukey post-hoc test). Data compiled from three independent experiments performed in duplicate each.

Supplemental Table 1

M&M section	Reagent or disposable	Vendor	Catalog Number	Concentration/Dose
Mice	Tamoxifen	Millipore Sigma	T5648	2 mg in 100 µL
	Peanut Oil	Millipore Sigma	P2144	N/A
	Lipopolysaccharides from Escherichia coli O111:B4 (LPS)	Millipore Sigma	L4391	250 µg/ 250 µL
Behavioral test	Y-maze	Stoelting, Wood Dale, IL	60180	
Cell Culture	Recombinant Human IL6 protein	R&D Systems	206-IL-200/CF	200 ng/mL
	Recombinant human IL6r alpha, CF	R&D Systems	227-SR-025/CF	100 ng/mL
	Lipopolysaccharides from Escherichia coli O111:B4 (LPS)	Millipore Sigma	L4391	2 µg/ml
	Recombinant Human TNF-alpha	R&D Systems	210-TA-020	10ng/ml
	EndoGRO-MV Complete Culture Media Kit	Millipore Sigma	SCME004	N/A
	DMEM/F12 Medium	ATCC	30-2006	N/A
	Endothelial Cell Growth Supplement	Sigma	E2759	40mg/mL
	Fetal Bovine Serum	Sigma	12306C	
	Penicillin-Streptomycin Solution, 100x	Corning	30-002-CI	1X
	Gelatin	Millipore Sigma	ES-006-B	0.1%
	0.05% Trypsin-EDTA	Gibco	25300054	1x
RNA isolation and RTqPCR	PrimeScript RT Master Mix	Takara	RR036B	1X
	TRIzol reagent	Invitrogen	15596018	1X
	iTaq Universal SYBR Green Supermix	Bio Rad	1725125	1X
TRAP	Avanti Polar Lipids, 1,2-diheptanlyl-sn-glycerol	Avanti Polar Lipids	NC9999043	300mM
	RNAsin Plus	Promega	PAN2615	40 U/ml
	Protein G beads	Thermo Fisher/Invitrogen	10004D	
	Ab for TRAP	Memorial Sloan Kettering CC	HTZGFP-19C8	
	Ab for TRAP	Memorial Sloan Kettering CC	HTZGFP-19F7	

	HBSS no calcium, mg, phenol red	Gibco	14175079	1X
	Complete mini edta free easy pack	Roche	4693159001	
	PhosStop	Roche	4906837001	
	Cyclohexamide	Sigma	C1988	100 µg/m
	DTT-biotech grade	VWR Life Sciences	97061-340	0.5 mM
	Potassium Chloride ACS	VWR Life Sciences	97061-566	350 mM
	HEPES Free Biotechnology grade	Sigma	H4034	1M
	Magnesium Chloride	Honeywell	63020	1M
	Diethyl pyrocarbonate (DEPC), 5ml	Sigma	D5758	
	Sodium Bicarbonate	Fisher Scientific	S233	4 mM
	(D) + Glucose	Acros	41095	
	Igepal	MP Biomedical	CA-630	1X
	Disposable pellet pestles with 1.5ml microtube	DWK Life Sciences	749520-0000	
	Cordless Pestle Motor	VWR Life Sciences	47747-370	
	Diamond Midi Centrifuge Tube, 5.0mL, PP, Separate Red Screw Cap, Graduated	Globe Scientific	111580	
	RNeasy Plus Micro Kit	Qiagen	74034	
	RNAse Away	Molecular Bioproducts	7002	

Supplemental table 2

Human RT-qPCR primer sequences

Primer name	Forward Sequence	Reverse Sequence
GAPDH	GTCTCCTCTGACTTCAACAGCG	ACCACCCTGTTGCTGTAGCCAA
IL6	TACCACTTCACAAGTCGGAGGC	CTGCAAGTGCATCATCGTTGTTC
SOCS3	CATCTCTGTCGGAAGACCGTCA	GCATCGTACTGGTCCAGGAACT
CXCL2	GGCAGAAAGCTTGTCTCAACCC	CTCCTTCAGGAACAGCCACCAA
CXCL10	GGTGAGAAGAGATGTCTGAATCC	GTCCATCCTTGGAAGCACTGCA
ICAM1	AGCGGCTGACGTGTGCAGTAAT	TCTGAGACCTCTGGCTTCGTCA
NAMPT	AGGGTTACAAGTTGCTGCCACC	CTCCACCAGAACCGAAGGCAAT
IL6R	AATACCTCGAGCCACAACCG	CAGCCAGCTATCTGGGGAAG
PECAM	CCAAGATAGCCTCAAAGTCGG	TCATAAGAAATCCTGGGCTGG
VWF	CCTTGAATCCCAGTGACCCTGA	GGTTCCGAGATGTCCTCCACAT
CDH5	GAAGCCTCTGATTGGCACAGTG	TTTTGTGACTCGGAAGAACTGGC
CLDN5	ATGTGGCAGGTGACCGCCTTC	CGAGTCGTACACTTTGCACTGC

Mouse genotyping primer sequences

Primer name	Forward Sequence	Reverse Sequence
Cdh5CreERT2	ACCAGCCAGCTATCAACTCG	TTACATTGGTCCAGCCACC
Rosa26fsTRAP	CTACAACAGCCACAACGTCTA	CAAACACAGCACCTTCTTCATC
SOCS3 flox	CGGGCAGGGGAAGAGACTGT	TCGACTGTCCTCGGTCAC